Supporting Information

DNA-templated silver and silver-based bimetallic clusters with remarkable and sequence-related catalytic activity toward 4-nitrophenol reduction

Weijun Zhou,[a,b] Youxing Fang,[a] Jiangtao Ren, [a]* and Shaojun Dong [a,b]*

Experimental Materials and Methods

Materials DNA samples (purchased from Sangon Biotechnology Co., Ltd. Shanghai, China) were dissolved in PB (20 mM Na_2HPO_4/NaH_2PO_4, pH 7.4) solution and quantified by UV absorbance at 260 nm. The extinction coefficients were obtained by summing extinction coefficients of individual bases in each sequence: ε(dA) = 15400 $M^{-1}cm^{-1}$, ε(dG) = 11500 $M^{-1}cm^{-1}$, ε(dC) = 7400 $M^{-1}cm^{-1}$ and ε(dT) = 8700 $M^{-1}cm^{-1}$. Sodium borohydride ($NaBH_4$) and silver nitrate ($AgNO_3$) were purchased from Sigma-Aldrich (St. Louis, MO, USA). All other reagents were analytically pure and used without pretreatment. Milli-Q water (specific resistance of 18.2 MΩ) was used throughout.

Instruments Cary 500 Scan UV–Vis–NIR spectrophotometer (Varian) and Fluoromax-4 spectrofluorometer (Horiba Jobin Yvon Inc., France) were used to collect the UV–Vis absorption spectroscopy and fluorescence spectra data. The UV-Vis results were carried out in a quartz cuvette with an optical path length of 1 cm. Both UV-Vis absorption and fluorescence spectra of clusters were measured under DNA templates concentration at 5 μM. Slit widths of fluorescence spectrophotometer for excitation and emission were both 10 nm. The luminescence decay curves were collected by a FLS920 spectrofluorometer with excitation wavelength at 375 nm. Transmission electron microscopy (TEM) images were recorded on a JEM-2100F high-resolution transmission electron microscope operating at 200 kV. Energy dispersive X-ray (EDX) spectra were measured with an XL30 ESEM FEG SEM (Philips, Netherlands) operating with an accelerating voltage of 20 kV. X-Ray photoelectron spectroscopy (XPS) analysis was implemented from an ESCALAB-MKII X-ray photoelectron spectroscope (VG Scientific, UK). Inductively coupled plasma mass spectrometry (ICP-MS) results were recorded by using a ThermoScientific iCAP6300.

Preparation of DNA-AgNCs 30 μM (final concentration, the same below) $AgNO_3$ was mixed with 5 μM DNA template in PB solution. After reacting for 1 hour, 30 μM $NaBH_4$ was added with vigorous shaking for 2 min, and then the reaction solution was incubated in dark for 6 hours. DNA-AgNCs were centrifuged under 5000 rpm for 10 min to eliminate large-size sliver nanoparticles before use.

Synthesis of bimetallic clusters Ag/Pd NCs, Ag/Au NCs and Ag/Pt NCs were synthesized by a GR reaction between AgNCs and H_2PdCl_4, $HAuCl_4$ and H_2PtCl_6 using AgNCs as sacrificial templates. Typically, different concentrations of H_2PdCl_4, $HAuCl_4$, and H_2PtCl_6 were added into the above-mentioned DNA-AgNC solutions with shaking for 5 min and incubated for 2 hours before use. The concentration ratios of $AgNO_3$ to noble metals were 30:1, 60:1 and 120:1, respectively.

HPLC-Mass Spectrometry Tandem HPLC-MS was performed in negative ion mode using Waters Acquity UPLC system equipped with a Q-TOF SYNAPT G2 High Definition Mass Spectrometer (HDMS) (Waters Crop., Manchester, UK) set to 2.0 kV capillary voltage and 35 V cone voltage. The source and desolvation temperatures were set to 120 and 150°C, respectively. Mass spectra were collected every second over the range 500-3000 m/z. The stationary phase of HPLC was 50mm x 4.6mm Kinetex C18 core-shell column with 2.6μm particle size and 100Å pore size (Phenomenex). All samples were run at room temperature at 0.4 mL/min. The mobile phase consisted of 16.3 mM triethylamine (TEA) and 400 mM 1,1,1,3,3,3-Hexafluoro-2-propanol (HFIP), solved in water and methanol, respectively. Clusters were purified using linear gradients from 10% to 50% methanol (1%/min).

Catalysis procedures 2 mM 4-NP was mixed with 235 mM fresh $NaBH_4$ and 30 μL AgNC or bimetallic

nanocluster. The final volume of mixture was 450 μL. Then 1 μL of the mixture solution was diluted to 1 mL and quickly measured by UV–Vis spectroscopy in a scanning range of 275–550 nm.

XPS, EDX and ICP-MS characterization of DNA-AgNCs and bimetallic clusters

Before the measurement, clusters were centrifugated by ultrafiltration centrifuge tubes with hyperfiltration membrane of 3 kDa to remove excess reagents. To meet the requirements of molecular cut off, A20C55-NC was chosen for the following experiments. XPS spectra of A20C55-NC and corresponding bimetallic clusters in Ag 3d were illustrated in Fig. S9. The Ag $3d_{5/2}$ and Ag $3d_{3/2}$ binding energy of A20C55-NC appeared at 367.6 and 373.7eV, respectively. The high resolution peaks of Ag 3d were deconvoluted into two pairs of doublets. The peaks at 367.93 and 373.96 eV were assigned to Ag^0 while peaks at 367.20 and 373.27 eV were attributed to the Ag^+ of AgNC, indicating the existence of both Ag (0) and Ag (I) on the surface of A20C55-NC. After the formation of bimetallic clusters, the relative ratio of Ag (0) and Ag (I) slightly altered. A little shift in the electron binding energy of Ag element was observed, owing to inter atomic charge redistribution caused by the valence band hybridization. XPS bands of Pd, Au and Pt were not obtained, for the contents of dopants were below the detection limit. The Ag 3d binding energy variation indicated the charge redistribution in Ag-Ag coupling due to noble metal doping.

Fig. S10 illustrated the EDX analysis of A20C55-NC and corresponding bimetallic clusters. The elements C, N, O, and P were supposed to be derived from A20C55 DNA template. The Na element may come from remnant PB buffer and Si element was ascribed to the silicon wafer. The elements Ag, Pd, Au and Pt derived with no doubt from AgNCs and bimetallic clusters. It is seen that the contents of sliver shown decreased trend in A20C55-NC, A20C55/$Pd_{1/30}$-NC, A20C55/$Au_{1/30}$-NC and A20C55/$Pt_{1/30}$-NC. ICP-MS results further revealed the accurate concentrations of Ag and doping metals in four types of clusters, which were consistent with EDX data (Table S3).

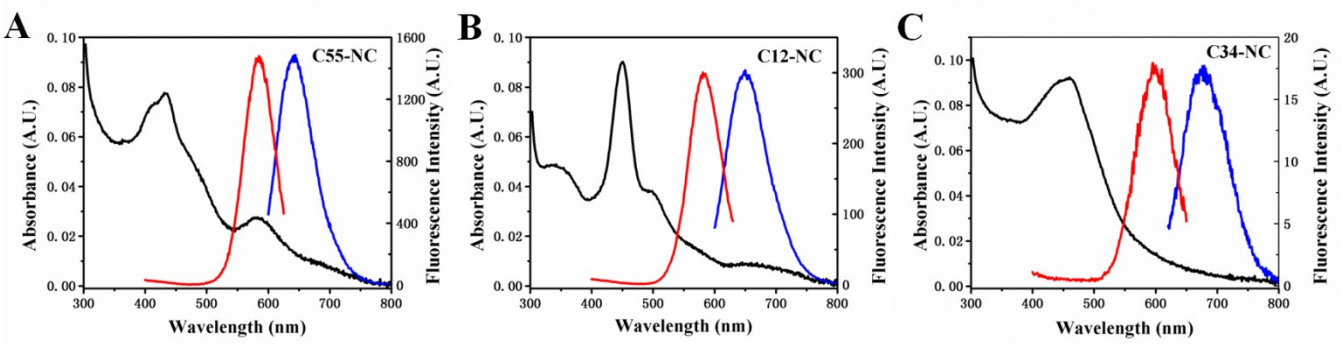

Fig. S1 UV-Vis absorption and fluorescence spectra of C55-NC (A), C12-NC (B) and C34-NC (C). The black, red and blue lines represent UV absorption, fluorescence excitation and emission spectra, respectively.

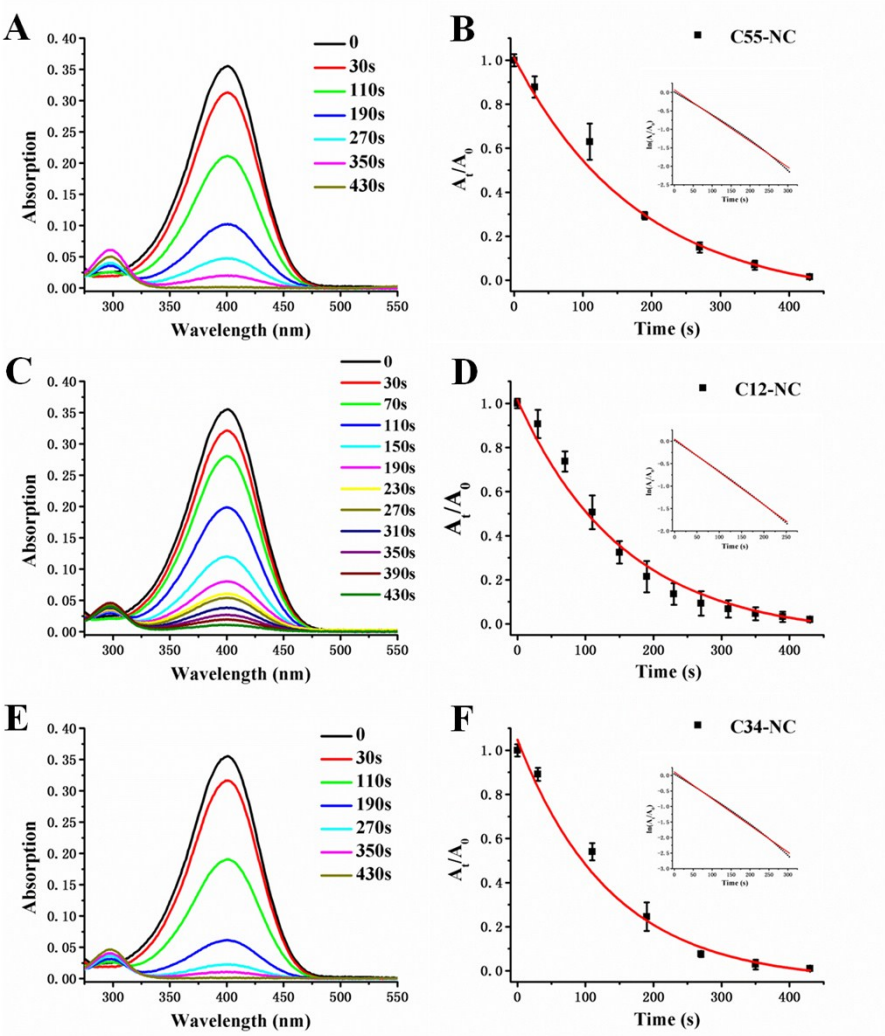

Fig. S2 UV-Vis absorption recorded during the reduction of 4-NP catalyzed by different DNA-AgNCs (A, C and E) and curves of absorbance ratio at 400 nm versus time (B, D and F). The insets show the plots of the $\ln(A_t/A_0)$ vs. the reaction time. A_t and A_0 are the absorption peak initially and at time t, respectively. Fig. A and B are for C55-NC; Fig. C and D are for C12-NC; Fig. E and F are for C34-NC. Error bars indicate the standard deviations of four measurements of independent samples for each time.

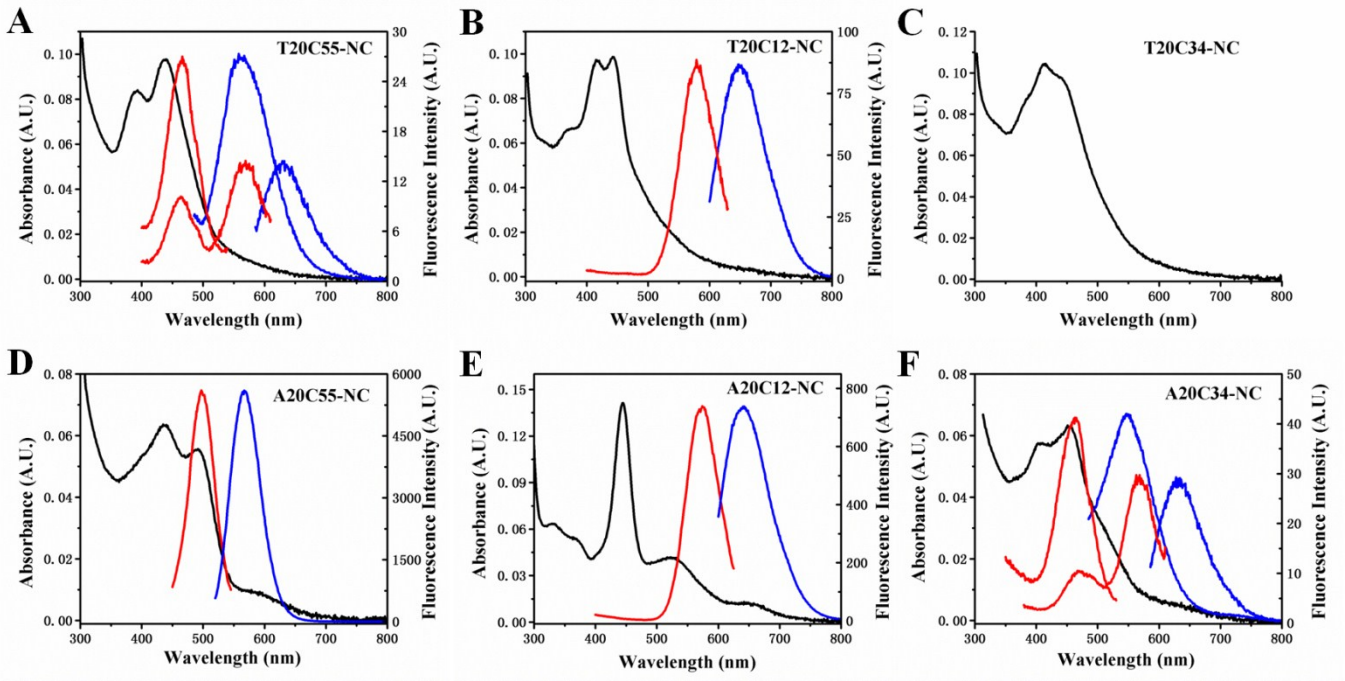

Fig. S3 UV-Vis absorption and fluorescence spectra of T20C55-NC (A), T20C12-NC (B), T20C34-NC (C), A20C55-NC (D), A20C12-NC (E) and A20C34-NC (F). The black, red and blue lines represent UV absorption, fluorescence excitation and emission spectra, respectively. T20C34-NC doesn't have fluorescence at all.

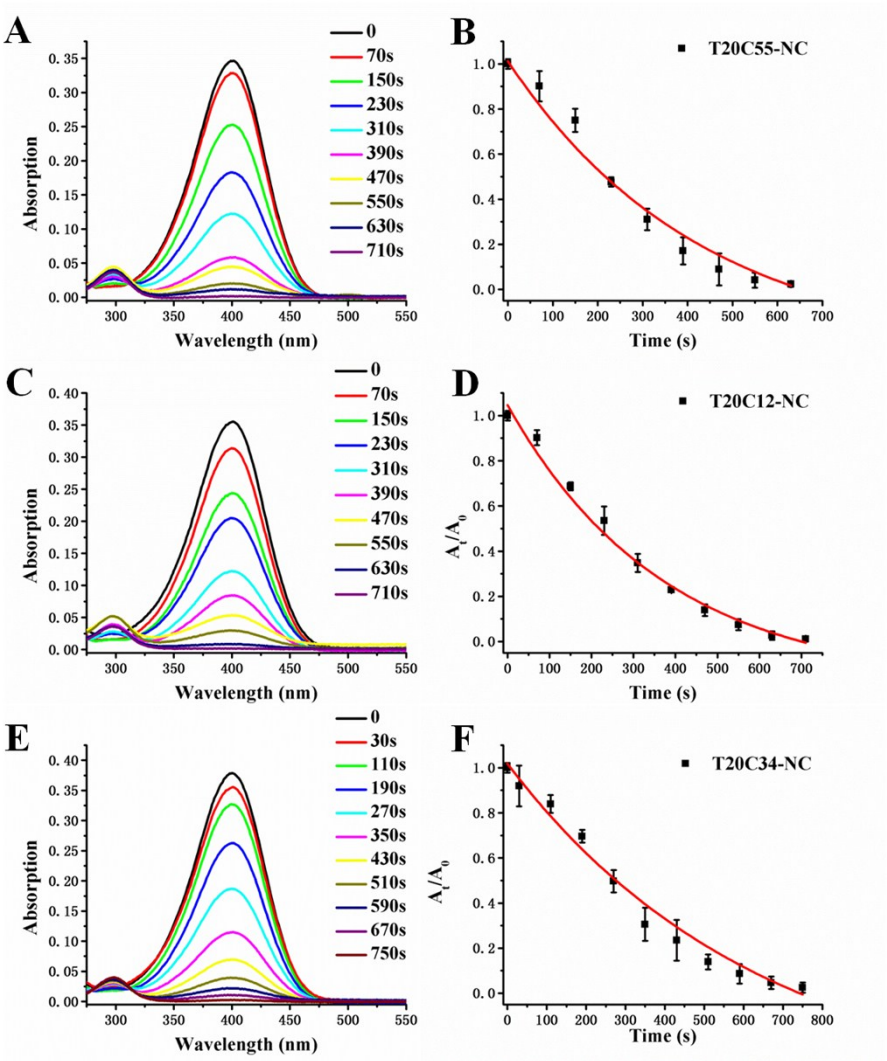

Fig. S4 (A, C and E) UV-Vis absorption recorded during the reduction of 4-NP catalyzed by different DNA-AgNCs. (B, D and F) Curves of absorbance ratio at 400 nm versus reaction time. A_t and A_0 represent the absorption peak initially and at time t, respectively. Fig. A and B are for T20C55-NC; Fig. C and D are for T20C12-NC; Fig. E and F are for T20C34-NC. Error bars indicate the standard deviations of four measurements of independent samples for each time.

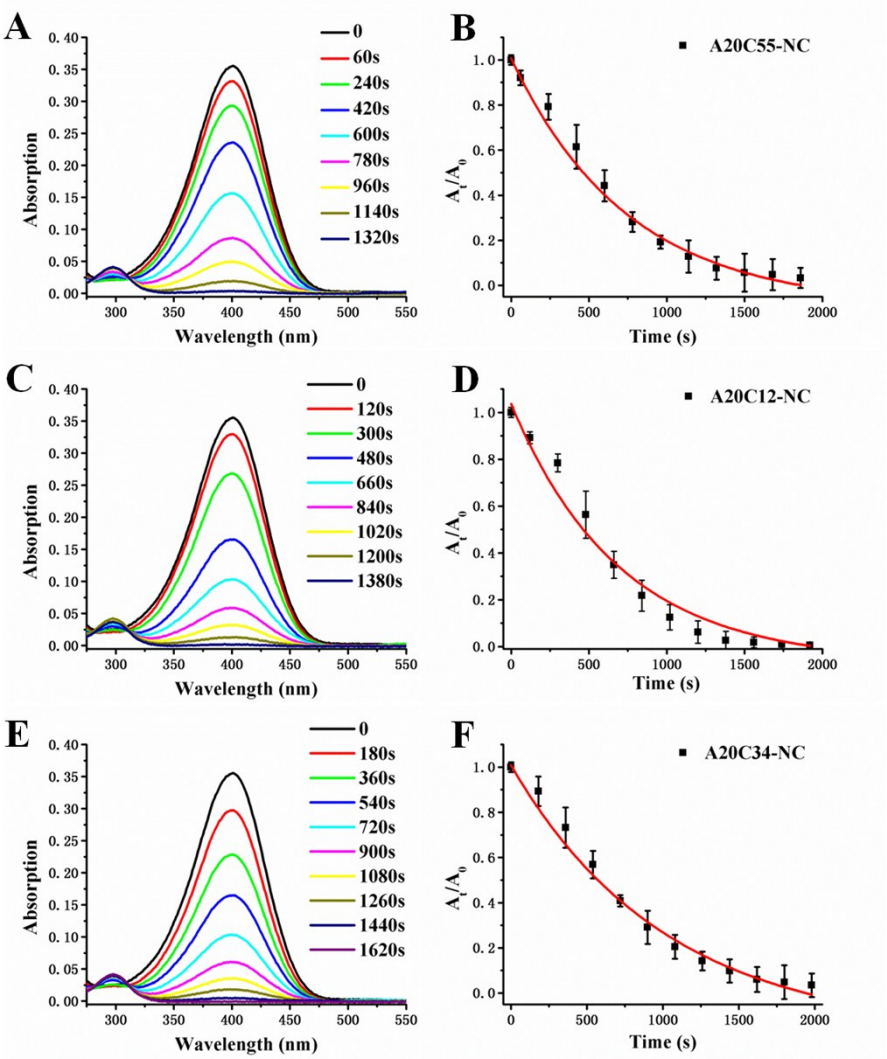

Fig. S5 (A, C and E) UV-Vis absorption recorded during the reduction of 4-NP catalyzed by different DNA-AgNCs. (B, D and F) Curves of absorbance ratio at 400 nm versus reaction time. A_t and A_0 represent the absorption peak initially and at time t, respectively. Fig. A and B are for A20C55-NC; Fig. C and D are for A20C12-NC; Fig. E and F are for A20C34-NC. Error bars indicate the standard deviations of four measurements of independent samples for each time.

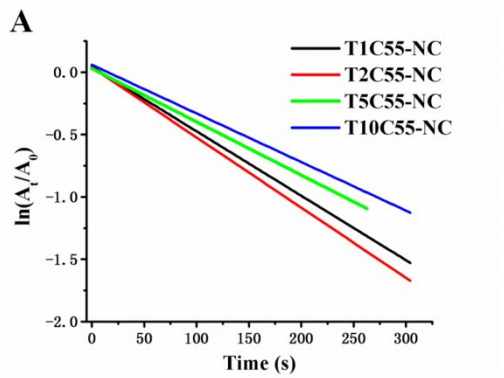

AgNC	k_{app} (10^{-3} s^{-1})
T1C55-NC	5.17
T2C55-NC	5.63
T5C55-NC	4.27
T10C55-NC	3.90

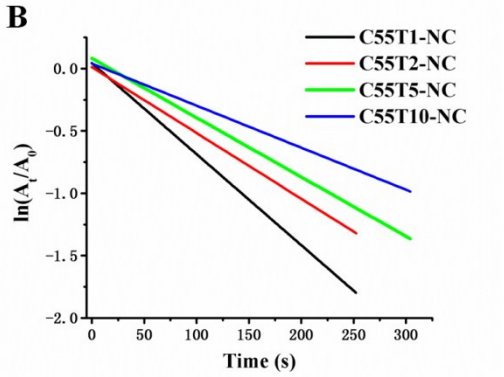

AgNC	k_{app} (10^{-3} s^{-1})
C55T1-NC	7.30
C55T2-NC	5.28
C55T5-NC	4.76
C55T10-NC	3.37

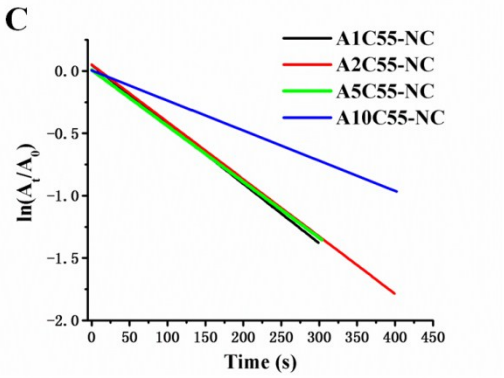

AgNC	k_{app} (10^{-3} s^{-1})
A1C55-NC	4.76
A2C55-NC	4.60
A5C55-NC	4.49
A10C55-NC	2.42

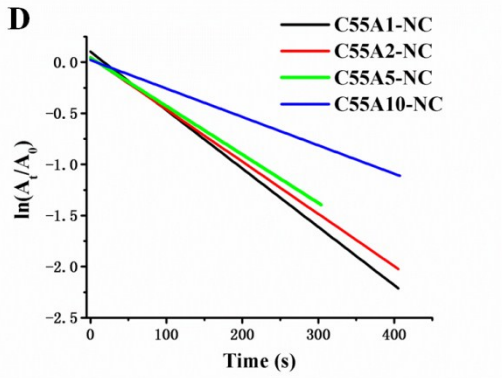

AgNC	k_{app} (10^{-3} s^{-1})
C55A1-NC	5.71
C55A2-NC	5.11
C55A5-NC	4.74
C55A10-NC	2.78

Fig. S6 The plots of the $\ln(A_t/A_0)$ vs. the reaction time and the apparent rate constants of 4-NP reduction catalyzed by (A) TnC55-NC, (B) C55Tn-NC, (C) AnC55-NC and (D) C55An-NC.

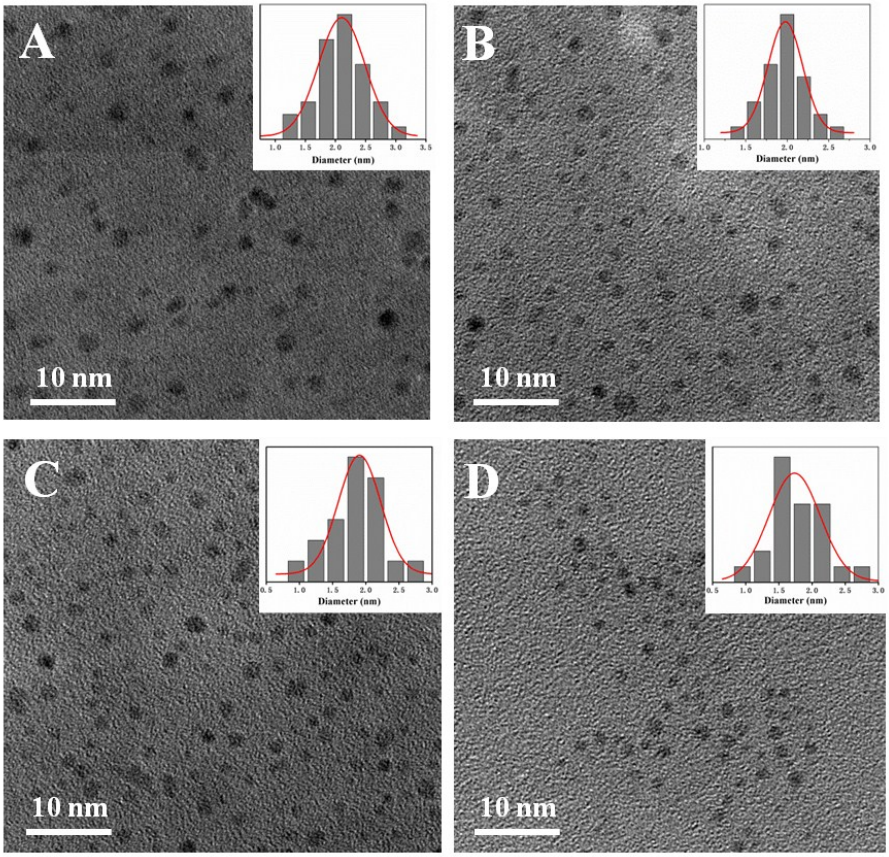

Fig. S7 TEM images and size distributions of C55-NC (A), C55/$Pd_{1/30}$-NC (B), C55/$Au_{1/30}$-NC (C) and C55/$Pt_{1/30}$-NC (D).

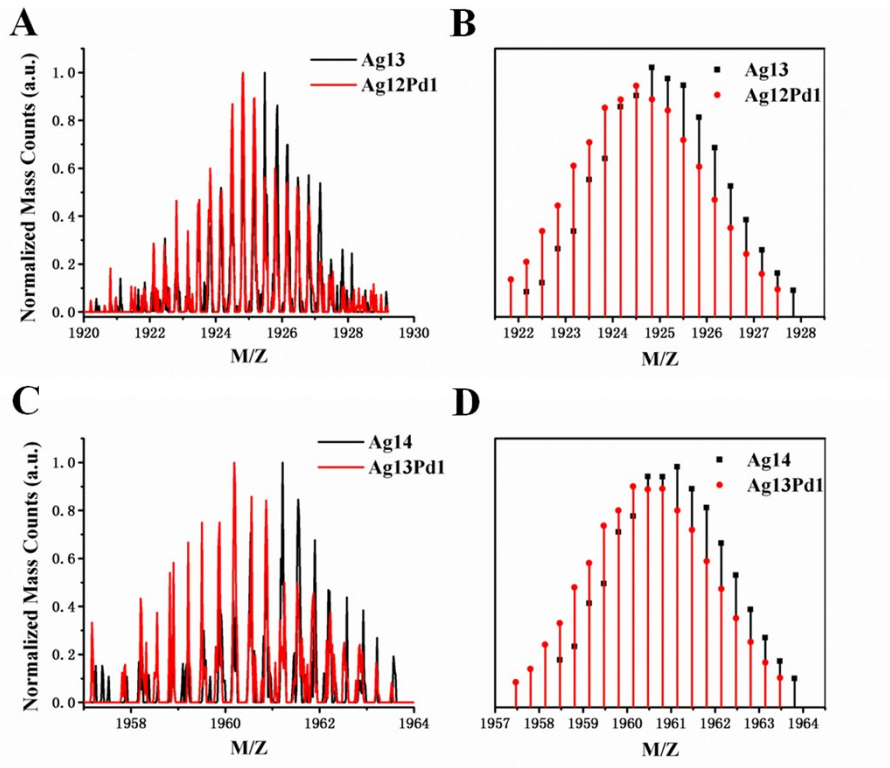

Fig. S8 The experimental (A and C) and simulated (B and D) isotopic patterns of different clusters. (A and B) $[Ag_{13}(C55)]^{3-}$ and $[Ag_{12}Pd(C55)]^{3-}$; (C and D) $[Ag_{14}(C55)]^{3-}$ and $[Ag_{13}Pd(C55)]^{3-}$.

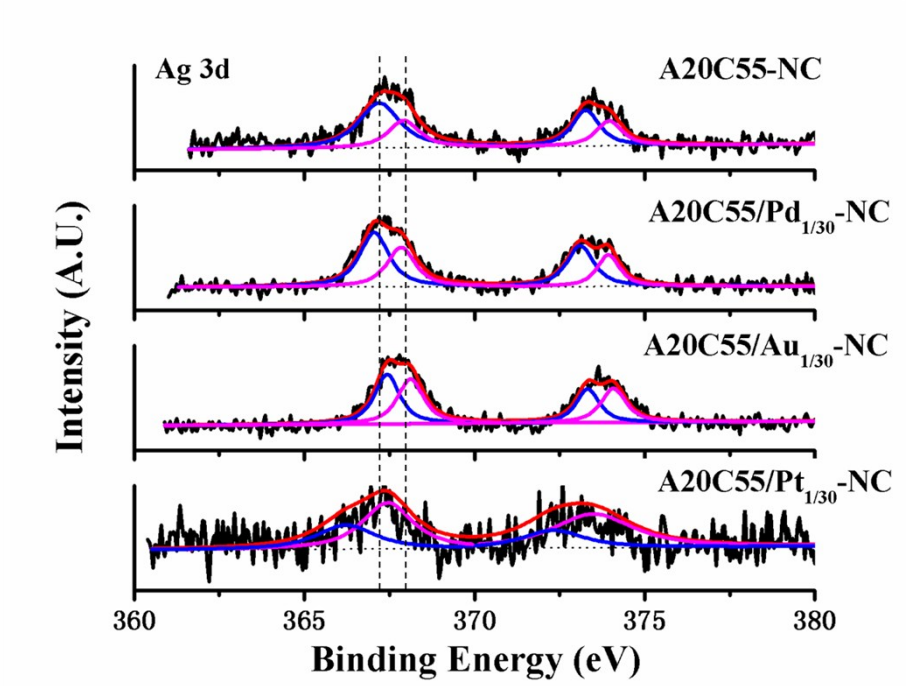

Fig. S9 Ag 3d XPS spectra of DNA-AgNC and bimetallic clusters deposited on a silica wafer.

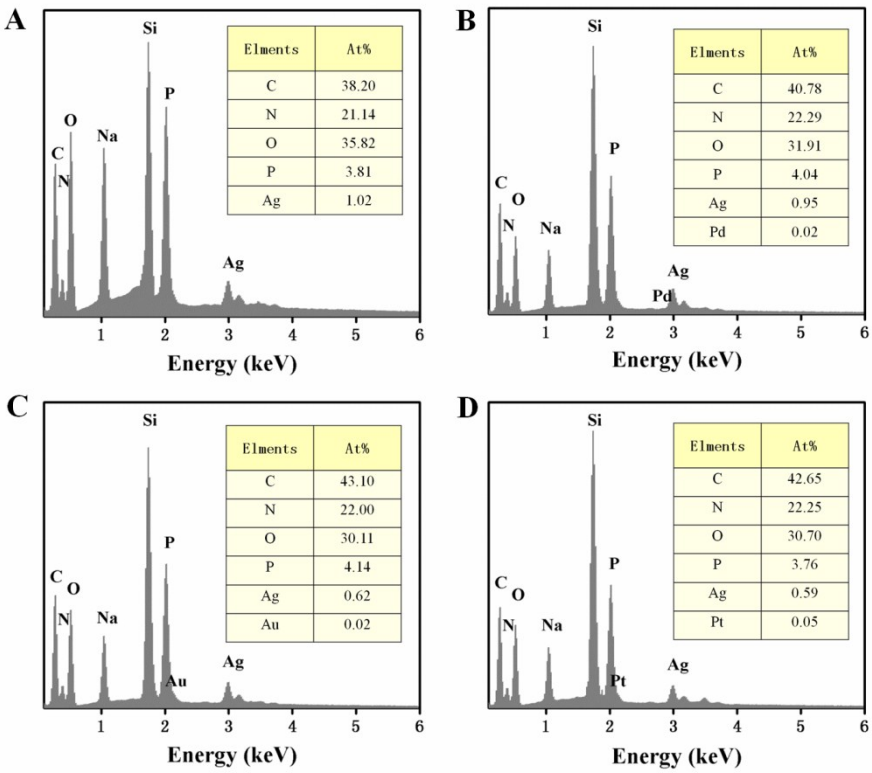

Fig. S10 EDX spectra and elements percentage of C55-NC (A), C55/$Pd_{1/30}$-NC (B), C55/$Au_{1/30}$-NC (C) and C55/$Pt_{1/30}$-NC (D).

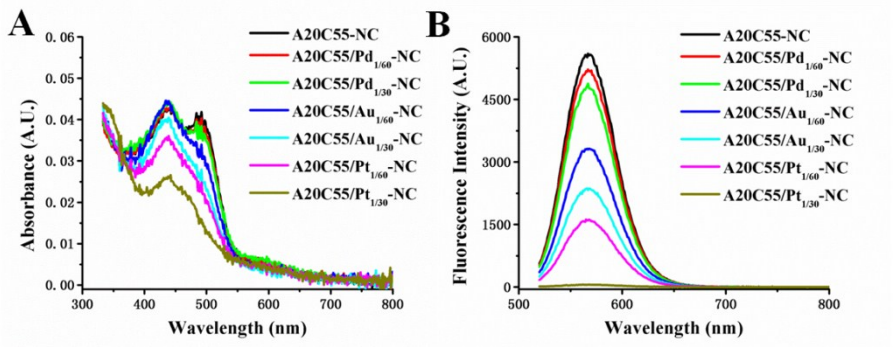

Fig. S11 UV-Vis absorption (A) and fluorescence spectra (B) variations of A20C55-NC after mixing with different concentrations of doping metals.

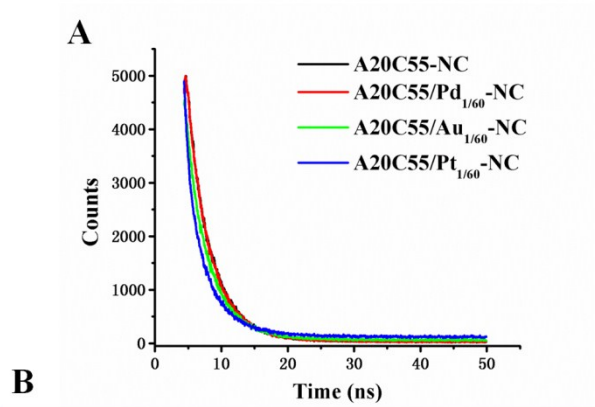

Samples	τ1 (ns)	w1	τ2 (ns)	w2
A20C55-NC	0. 850	0. 890	3. 650	0. 110
A20C55/$Pd_{1/60}$-NC	1. 545	0. 516	3. 715	0. 484
A20C55/$Au_{1/60}$-NC	1. 094	0. 730	3. 667	0. 270
A20C55/$Pt_{1/60}$-NC	1. 034	0. 927	3. 756	0. 073

Fig. S12 (A) Fluorescence emission decays of A20C55-NC and bimetallic clusters. (B) Lifetimes of the two exponentials required to fit the fluorescence decay curves.

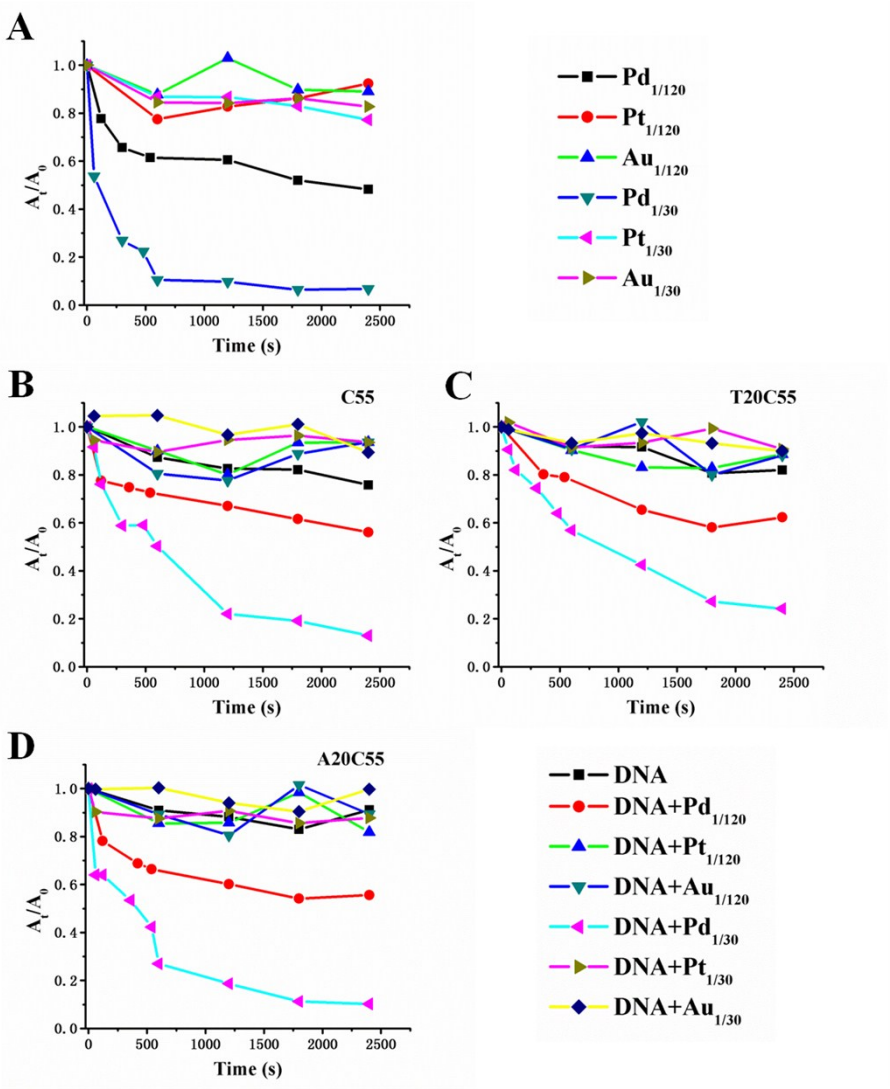

Fig. S13 Curves of absorbance ratio at 400 nm versus time during the reduction of 4-NP catalyzed by different noble metals (A), or metals mixed with DNA templates, C55 (B), T20C55 (C) or A20C55 (D). A_t and A_0 represent the absorption peak initially and at time t, respectively.

Oligo name	DNA Sequence (5'→3')
C55	CCCCCTAATTCCCCC
C12	CCCCCCCCCCCC
C34	CCCCTAATTCCC
A20C55	AAAAAAAAAAAAAAAAAAACCCCCTAATTCCCCC
A20C12	AAAAAAAAAAAAAAAAAAACCCCCCCCCCCC
A20C34	AAAAAAAAAAAAAAAAAAACCCCTAATTCCC
T20C55	TTTTTTTTTTTTTTTTTTTCCCCCTAATTCCCCC
T20C12	TTTTTTTTTTTTTTTTTTTCCCCCCCCCCCC

T20C34	**TTTTTTTTTTTTTTTTTTTTCCCCTAATTCCC**
T1C55	**TCCCCCTAATTCCCCC**
T2C55	**TTCCCCCTAATTCCCCC**
T5C55	**TTTTTCCCCCTAATTCCCCC**
T10C55	**TTTTTTTTTTCCCCCTAATTCCCCC**
C55T1	**CCCCCTAATTCCCCCT**
C55T2	**CCCCCTAATTCCCCCTT**
C55T5	**CCCCCTAATTCCCCCTTTTT**
C55T10	**CCCCCTAATTCCCCCTTTTTTTTTT**
A1C55	**ACCCCCTAATTCCCCC**
A2C55	**AACCCCCTAATTCCCCC**
A5C55	**AAAAACCCCCTAATTCCCCC**
A10C55	**AAAAAAAAAACCCCCTAATTCCCCC**
C55A1	**CCCCCTAATTCCCCCA**
C55A2	**CCCCCTAATTCCCCCAA**
C55A5	**CCCCCTAATTCCCCCAAAAA**
C55A10	**CCCCCTAATTCCCCCAAAAAAAAAA**

Table S1 DNA strands used in this study.

AgNC	λ_{ex} (nm)	λ_{em} (nm)	Relative intensity
C55-NC	580	645	106
C12-NC	580	650	21.6
C34-NC	600	672	1.3
A20C55-NC	500	567	400
A20C12-NC	580	645	52.5
A20C34-NC	465 565	545 628	3 2
T20C55-NC	465 565	558 630	1.9 1
T20C12-NC	580	648	6.2
T20C34-NC	—	—	—

Table S2 The fluorescence excitation, emission and relative fluorescence intensity of different DNA-AgNCs. Fluorescence intensity of T20C55-NC at 630 nm was standardized as 1.

Samples	Ag ($ng\ mL^{-1}$)	Pd ($ng\ mL^{-1}$)	Au ($ng\ mL^{-1}$)	Pt ($ng\ mL^{-1}$)
A20C55-NC	1640			
A20C55/$Pd_{1/60}$-NC	1554	32		
A20C55/$Au_{1/60}$-NC	1501		58	
A20C55/$Pt_{1/60}$-NC	1493			47

Table S3 Mass concentrations of Ag and doping metals obtained from ICP-MS.

Samples	k_{app} (10^{-3} s^{-1})	k_{nor} ($L \cdot g^{-1} \cdot s^{-1}$)	References
C55-NC	6.98	63.84	This work
C55/$Pd_{1/30}$-NC	16.43	155.39	
C55/$Au_{1/30}$-NC	9.65	92.85	
C55/$Pt_{1/30}$-NC	14.58	142.01	
AgNC	0.35	—	J. Colloid. Interf. Sci. 2018, 529, 444
Ag NC/GSH-rGO	9.17	2.64	
CPL-Ag NCs	1.83	—	RSC Adv. 2016, 6, 14247
AgNP-PG	5.50	1.38	Langmuir 2013, 29, 4225
Ag NPs@PGMA-SH	3.94	4.38	Ind. Eng. Chem. Res. 2015, 54, 6480
EPS–Ag NPs	1.26	0.047	RSC. Adv. 2015, 5, 69790
AgNP/XAD-4	13.90	1.948	RSC Adv. 2014, 4, 33366
AgNP-PPA	15.46	436.00	Langmuir, 2016, 32, 7383
AgNP-GSH	17.04	77.70	
AgNP-BSA	1.53	3.50	

Table S4 Comparison of various catalysts for catalyzing the reduction of 4-NP.